Mergers, Interactions, and The Fueling of Starbursts

J. E. Hibbard[1]
Institute for Astronomy, University of Hawaii
hibbard@uhifa.ifa.hawaii.edu

To appear in *"Star Formation, Near and Far"*,
The 7^{th} Annual Astrophysics Conference in Maryland,
S.S. Holt & L.G. Mundy, editors.

Electronic version of this paper is available at:
http://www.ifa.hawaii.edu/~hibbard/MdConf/

UNIVERSITY OF HAWAII
INSTITUTE FOR ASTRONOMY
2680 Woodlawn Drive
Honolulu, Hawaii 96822 USA

[1] Hubble Fellow

Mergers, Interactions, and The Fueling of Starbursts

John E. Hibbard

Institute for Astronomy
2680 Woodlawn Drive
Honolulu, Hawai'i 96822

Abstract. The most active starbursts are found in galaxies with the highest IR luminosities, with peak star formation rates and efficiencies that are over an order of magnitude higher than in normal disk systems. These systems are almost exclusively on-going mergers. In this review I explore the conditions needed for interactions to experience such a phase by comparing two systems at similar stages of merging but quite different IR luminosities: NGC 4038/9 and Arp 299. These observations show that the most intense starbursts occur at the sites with the highest gas densities, which is a general result for IR luminous mergers. Observations and theory both suggest that the strength of the merger induced starburst depends on the internal structure of the progenitors, the amount and distribution of the gas, and the violence of the interaction. In particular, interactions involving progenitors with dense bulges, gas-rich disks, and/or a retrograde spin are expected to preferentially lead to large amounts of gaseous dissipation, although the interplay between these parameters is unknown. A major outstanding question is how the effects of feedback alter these conclusions.

INTRODUCTION

While galaxies showing both peculiar morphologies and signs of global youth have been known for decades (e.g. [1–3]), it was not until a classic study on the UBV colors of peculiar galaxies by Larson & Tinsley in 1978 [4] that the study of starbursts in interacting galaxies began in earnest. In that seminal work the authors showed that the disturbed systems from the Arp *Atlas of Peculiar Galaxies* [5] had a larger spread in colors and significantly bluer colors than a comparison sample of normal Hubble types. The Toomres [6] had recently demonstrated quite convincingly that gravitational interactions provide a natural explanation for many of the types of peculiarities exhibited by the systems in Arps atlas, and Larson & Tinsley posited that such interactions induce small bursts ($\sim$ 1-5% by mass) of star formation within the host(s). They were able to explain the color distribution of the Arp sys-

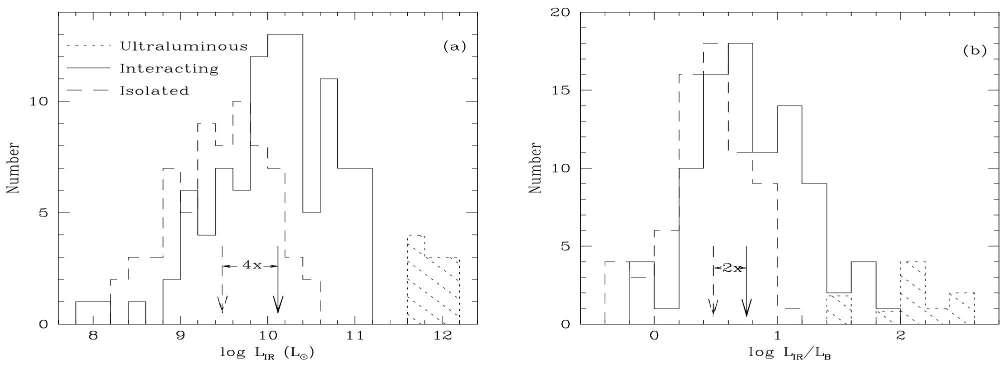

FIGURE 1. Histograms of L_{IR} and L_{IR}/L_B for isolated, interacting, and infrared bright systems. The isolated and interacting samples were chosen optically, independent of their infrared properties. Arrows indicate their means. These plots show that while the brightest IR emitting systems are interacting, many interacting systems are not IR bright. From Bushouse, Lamb & Werner 1988 [8].

tems with burst models of varying strength and age superimposed upon an underlying host with normal colors.

Much subsequent work has supported this suggestion [7]. The consensus is that interacting galaxies as a class have mean levels of star formation that are factors of 2–5 higher than normal spirals for optically selected samples, or 2–20 times higher for samples selected on the basis of IR luminosity. This point is illustrated in Figure 1 [8], which compares the IR luminosities of an optically selected samples of isolated and interacting galaxies. Also shown are the values for a sample of ultraluminous infrared (ULIR[2]) galaxies which are known to be on-going mergers [9]. Similar results have been derived using other measures of star formation, finding that interactions serve primarily to concentrate moderately enhanced star formation into the central regions of galaxies rather than to globally raise the star formation rate (e.g. [10–13]).

Figure 1 illustrates several other points. The first is that none of the isolated systems have $L_{IR} > 3 \times 10^{10} L_\odot$ or $L_{IR}/L_B > 15$. At these levels almost all galaxies are interacting or merging [9,14,15]. In fact, IR luminosity appears to be the most efficient way to select interacting systems: while the overall peculiar fraction of optically selected samples is around 9% [16], the fraction of morphologically peculiar galaxies approaches 90% or higher at IR luminosities above $5 \times 10^{11} L_\odot$ (see [17] and references therein). The second is that many systems in the interacting sample do *not* exhibit enhanced levels of star formation. So while the most luminous IR sources are almost invariably mergers, not all mergers are luminous IR sources.

IR luminosity is believed to be directly related to the number of hot stars present, as the dust absorbs the UV photons from these stars and reradiates

---

2) $L_{IR} > 3 \times 10^{11} L_\odot$ in this case, although other definitions are used

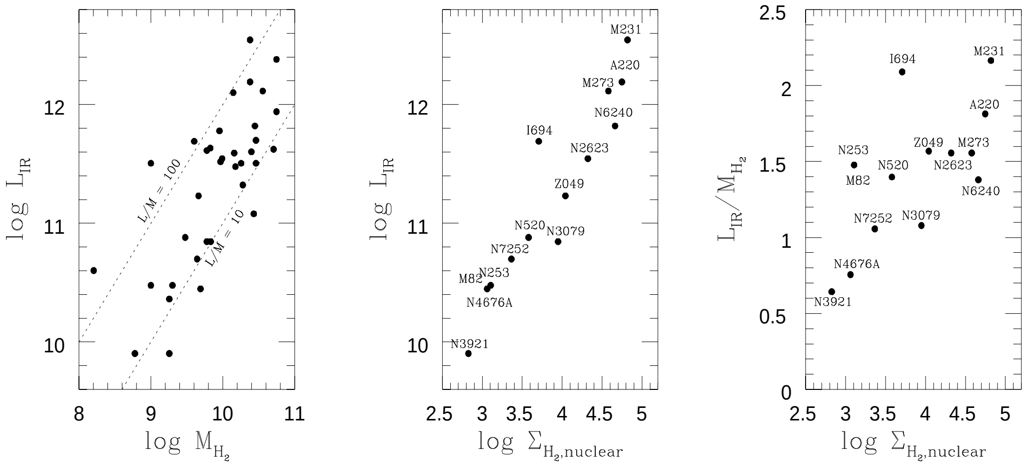

FIGURE 2. **(a)** total IR luminosity vs. derived H_2 mass for all objects observed at OVRO. Normal spirals fall below the L/M=10 line. **(b)** L_{IR} vs. the molecular gas column density averaged over a 1 kpc diameter region ($\Sigma_{H2,nuclear}$) for the 12 objects observed with sufficient resolution. **(c)** SFE vs. $\Sigma_{H2,nuclear}$. From Yun & Hibbard, in preparation.

them in the IR [14,15]. It can therefore be used as a measure of the massive star formation rate (MSFR; $M > 5M_{\odot}$) [18]. The IR luminous systems are both gas-rich and dusty [9,19,20], and most of their bolometric luminosity emerges in the far IR [9,17]. While there has been a long-standing debate over whether the most luminous systems are instead powered by an obscured AGN (see e.g. [13,21]), this ambiguity is mostly at the highest IR luminosities, and the majority are believed to be predominantly powered by starbursts (see reviews by [7,22]). The popular picture which has emerged is that two gas rich systems undergo a close interaction, which leads to orbital decay and eventual merging. The gas is compressed, dissipates and moves inward, stimulating a circumnuclear starburst. Dust, which is coupled to the gas, absorbs much of the UV radiation and re-radiates it in the IR. This high level of star formation quickly subsides as the burst consumes the available gas.

But do all mergers experience a strong burst of star formation? If not, what are the deciding factors? These are the issues I will discuss in this review.

Quantifying the Star Formation Activity

Although star formation activity has historically been defined by some absolute quantity such as IR luminosity, it would be preferable to use a relative measure which compares the total SFR to the the size of the system. In this way we can address whether star formation proceeds in an inherently different manner at these luminosities, or if it is a scaled up version of processes taking place at lower luminosities. Blue luminosity is frequently used as a substitute for the stellar mass (e.g. Fig. 1b), although this interpretation is wrought with uncertainties due to the presence of young stars and large amounts of dust.

L_{IR}/L_K is a more useful measure, although L_K is still affected by the presence of red AGB stars.

A popular normalization introduced by millimeter astronomers is the ratio of the IR luminosity to the molecular gas mass (L_{IR}/M_{H2}), where M_{H2} is estimated from measurements of the CO line. This ratio is termed the "star formation efficiency" (SFE) [20,23,24] as it represents in some global sense the number of massive stars formed per giant molecular cloud. Since L_{IR} ~MSFR [18], the SFE is inversely related to the gas depletion time, and is thus equivalent to the more classical definition of a starburst (*i.e* $\Delta t_{burst} << H_o^{-1}$).

Many studies have evaluated the SFE in merging galaxies concluding that ULIR mergers are forming stars up to an order of magnitude more efficiently than normal spirals (see Figure 2 and [17]). While there is some question as to whether the Galactic conversion factor between CO and H_2 applies in merging galaxies [19,25,26], the expected variation leads to an overestimate of the molecular gas and therefore underestimates the actual SFEs. It therefore seems hard to escape the conclusion that massive stars are being formed at a higher rate for a given amount of cold gas than in quiescent systems, although the exact level of the enhancement is uncertain.

The Tails of Two Mergers

To understand how this efficient mode of star formation is triggered, it is instructive to compare two nearby mergers at apparently similar stages of merging but at two quite different levels of star formation activity. The mergers I will examine are "The Antennae" (NGC 4038/9, Arp 244; V_o=1630 km s^{-1}) and Arp 299 (NGC 3690/IC 694; V_o=3080 km s^{-1}). Both the tidal structure and inner disks of these systems are shown in Figure 3 along with distribution of the cold gas components.

The evidence that these systems are at a similar stage of merging is the following: both have a long tidal tails (130 kpc for NGC 4038/9 assuming a distance of 25 Mpc; 180 kpc for Arp 299 assuming a distance of 48 Mpc), suggesting several hundred Myr since first orbital periapse ($\gtrsim$500 Myr for NGC 4038/9; $\gtrsim$700 Myr for Arp 299); the disks of their progenitors are highly distorted and in physical contact, yet still distinct; and their nuclei are still well separated (8 kpc and 4 kpc, respectively). Both systems have similar CO distributions (Fig. 3c-d), with concentrations of cold molecular gas near both nuclei and a significant concentration at the region of disk overlap. Despite these similarities, Arp 299 is almost an order of magnitude more luminous in the infrared than NGC 4038/9, indicating a much higher MSFR (see Table 1).

In Table 1 we use NIR flux measurements [27,28] to divide the IR luminosity among the various components. This comparisons shows that a major difference between the systems is in the amount of nuclear star forming activity: in NGC 4038/9, the overlap region is the most active star forming region, both in terms of the MSFR and the SFE. In Arp 299, on the other hand, the overlap region has similar properties as that in NGC 4038/9, but both nuclei outshine

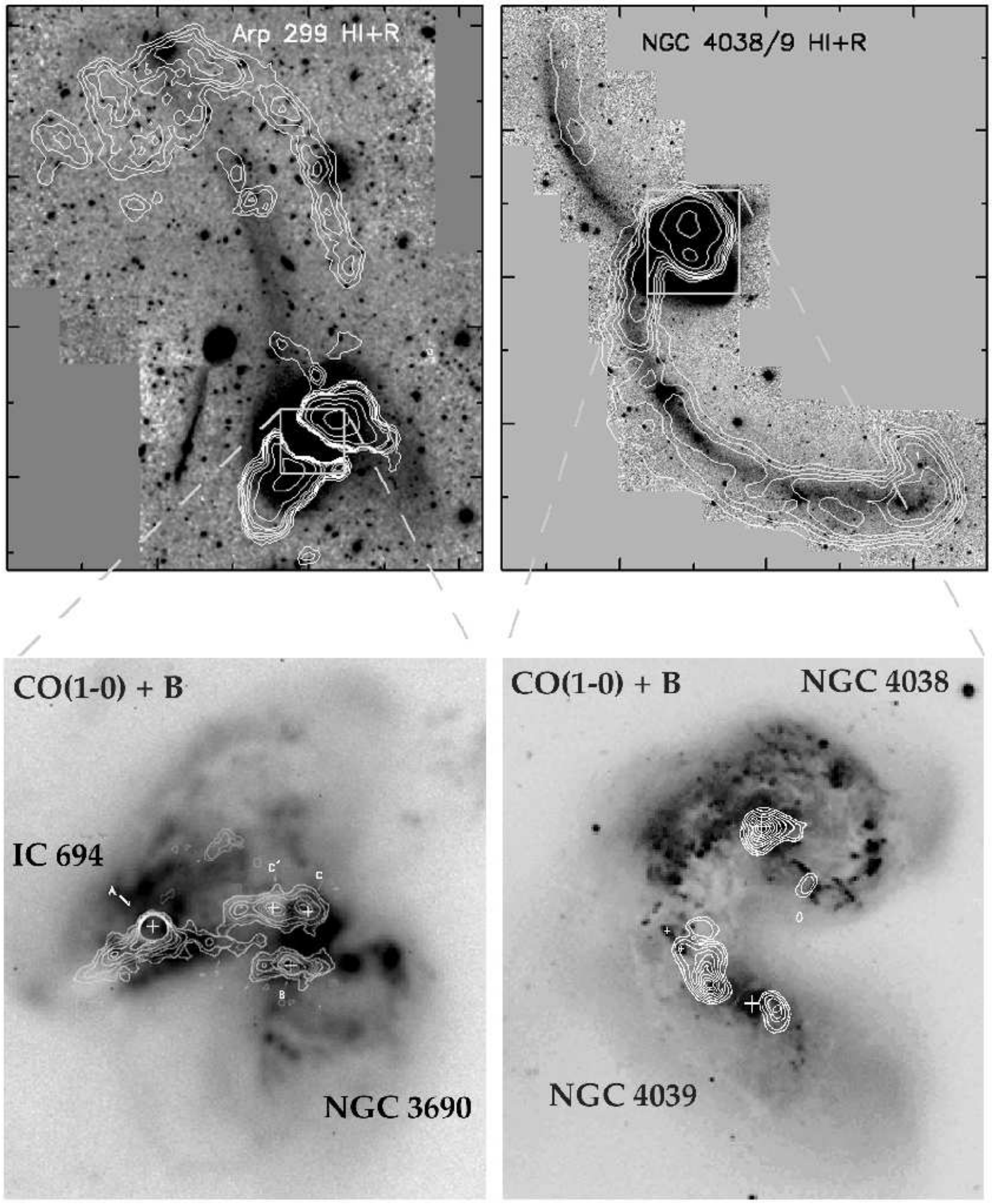

FIGURE 3. Two on-going mergers. (a)&(c) NGC 4038/9 and (b)&(d) Arp 299. In the upper two panels, a deep R-band image of the entire system is shown with VLA H I contours overlaid, while in the lower two panels a B-band image of the inner regions is shown with OVRO ^{12}CO(1-0) contours overlain. The optical data were obtained by the author; the VLA data are from Hibbard & Yun 1996 [31] (Arp 299) and Hibbard & van der Hulst in preparation (NGC 4038/9); the OVRO data are from Aalto *et al.* 1997 [32] (Arp 299) and Stanford *et al.* 1990 [33] (NGC 4038/9). These systems appear to be at similar stages of merging, with their disks in contact and their nuclei still separate.

TABLE 1. Properties of Star Forming Regions in Arp 299 & NGC 4038/9.

	L_{IR} [a] ($\times 10^{10} L_{\odot}$)	M_{H2} [b] ($\times 10^{9} M_{\odot}$)	L_{IR}/L_K	MSFR ($M_{\odot}\mathrm{yr}^{-1}$)	Σ_{H2} ($M_{\odot}\mathrm{pc}^{-2}$)	SFE ($L_{\odot} M_{\odot}^{-1}$)
IC694	49.8	4.0	—	31	27,000	124
N3690	24.5	1.0	—	15	4,900	245
overlap	4.7	2.0	—	3	3,400	24
Arp 299	79.0	7.0	31	49	27,000	113
N4038	2.0	0.8	—	1	1,200	25
N4039	0.04	0.2	—	0	540	2
overlap	7.8	1.2	—	5	1,350	65
N4038/9	9.8	2.0	13	6	1,350	49

[a] L_{IR} is split between components using 15μm ISOCAM measurements for NGC 4038/9 [27], and 32μm measurement for Arp 299 [28].
[b] From OVRO CO observations of NGC 4038/9 [33] and Arp 299 [34].

this region by large amounts. We note that observations argue against an energetically dominant AGN in any of the nuclei [13,27–29] (but see [30]).

Similar differences are seen in the column densities of molecular gas: there is five times as much gas in the central kpc of the nuclei of Arp 299 as in NGC 4038/9. As a result, the peak column densities are over an order of magnitude higher in the nuclei of Arp 299 as in the nuclei of NGC 4038/9 or the overlap regions. The tight correlation between Σ_{H2} and L_{IR} shown in Fig. 2 shows this to be a general result for mergers over a broad range of IR luminosity [20]. While it is still possible that M_{H2} has been overestimated [25,26] a similarly tight correlation exists between L_{IR} and L_{HCN}, as well as between SFE and L_{HCN}/L_{CO} [35], showing that the fraction of gas at very high densities ($n > 10^5 \mathrm{cm}^{-3}$) is greatly increased in ULIR systems. As these fractions are much higher than those found in normal spirals, this indicates that MSFR is intricately linked to the amount of gaseous dissipation [19,26,36].

It therefore seems that in order to understand how such efficient periods of star formation are induced, we need to understand how so much gas attains such high gas densities. Most phenomenological scenarios of star formation predict that the MSFR and the SFE are proportional to the gas density to some power (e.g. [37,38]), although they do not address in detail when and where such densities are attained. For this, we turn now to results from numerical simulations.

Lessons from Simulations

Ever since a dissipational component was first included in numerical simulation of interactions it has been clear that large amounts of gas can be efficiently driven into the central regions [39–41]. In this section I examine individual models for clues as to what parameters play the largest role in driving gas to high densities. This is not intended to be a review of all the simulations (for

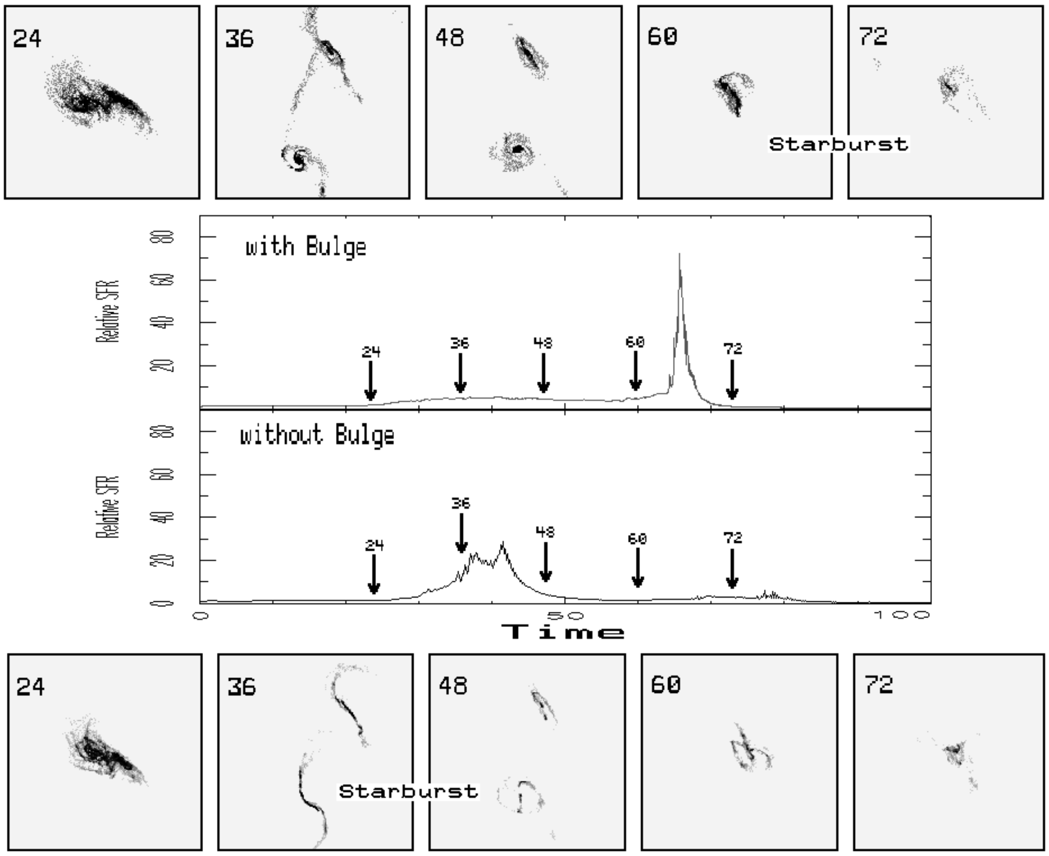

FIGURE 4. Time history of two interaction induced starbursts. In the bottom sequence, the lack of a dense bulge allows strong bar-induced inflows to develop early in the encounter. The relatively mild starburst which ensues consumes much of the available gas supply, leading to a less extreme burst at the final merger. Adapted from Mihos & Hernquist [43].

that see [42]), but rather an assessment of the results which might have the most relevance for understanding the observations discussed above.

Progenitors: A very interesting result to emerge from the numerical studies is that the progenitor structure ought to play a dominant role in the star formation history (SFH) [43,44]. This is illustrated in Figure 4. In the upper sequence the presence of a bulge stabilizes the disks against bar formation, lowering the pre-merger star formation levels, but leaving more gas in the progenitors to fuel a strong starburst when they finally merge. Because of the peaked appearance, it is tempting to associated this SFH with the ULIR systems, but it is important to realize that the vertical axis is a *relative* SFR, and the absolute SFR between the two curves could differ due to other factors (see below). Indeed, the fact that Arp 299 is so luminous while the nuclei are still well separated suggests that it follows the lower SFH in Fig. 4. This interpretation is supported by the H I observations, which suggests two late type progenitors [45]. NGC 4038/9 on the other hand appears to have one late type (NGC 4038) and one earlier type (NGC 4039) progenitor [46], and may have a SFH more like the upper curve in Fig. 4, with its most active star forming period still to come. These considerations suggest that while a dense bulge may push certain systems into the ULIR regime, it need not be a strict requirement. They also point to the need for better constraints on the past and future star forming histories to facilitate comparisons with models.

Gas content: There is over three times as much molecular gas in Arp 299 than NGC 4038/9, although the relative gas contents are similar (M_{H2}/L_K=0.5, 0.4). Could this be responsible for the different levels of activity? Clearly the level of star formation must be closely connected to the amount of fuel available, but plots of SFE or L_{IR} *vs.* M_{H2} show notoriously large amounts of scatter (e.g. Fig. 2a). So while the gas content may help shift the SFR upward for some systems (see Gao *et al.* these proceedings), high gas mass alone is not a sufficient condition for fueling an ULIR phase. Olson & Kwan [47] conducted one of the few simulations to explore the effects of different gas masses and distributions. Using a code in which the SFR is proportional to the cloud collision rate, they find that doubling the gas content in one of the disks in a disk-disk merger doubles the SFR, therefore keeping the SFE (=SFR/M_{gas}) constant, while splitting the same amount of gas between two galaxies leads to a 30% higher SFR and SFE than putting it all into one of the system. This suggests that how the gas is distributed and how it collides is as important as how much gas is present. These studies should be continued with a wider range of encounter parameters.

Spin geometries: The two systems under consideration here differ in their spin geometries, with Arp 299 undergoing a prograde-retrograde encounter [45,48] and NGC 4038/9 undergoing a prograde-prograde encounter [46]. Since retrograde encounters fail to raise strong tails [49], there will be more gas left in the inner regions at the late stages of merging where it will be violently perturbed as the encounter progresses. The simulations of Barnes & Hernquist [49] show that the fraction of gas at high densities depends on encounter geometry, with retrograde encounters leading to higher quantities of dense gas than prograde encounters. In Arp 299, the highest gas column densities are found in the nucleus of the disk experiencing the retrograde encounter (IC 694). Mihos & Hernquist [43,44] also evaluated the effects of spin geometry, and while they showed that it had a much less dramatic effect on the SFRs than progenitor structure, geometry still made a difference of about a factor of two in the relative SFRs. If there is either a threshold to the onset of very efficient star formation activity, or if SFE is a function of the fraction of the gas at very high densities, it is possible that spin geometry plays a role beyond that attributed to it in these studies.

The reality is that all of the factors are probably playing a part, although in what combination and order of importance is not clear. Continued parameter studies are needed in concert with detailed observations of individual systems in order to discriminate between the different processes. It is also important

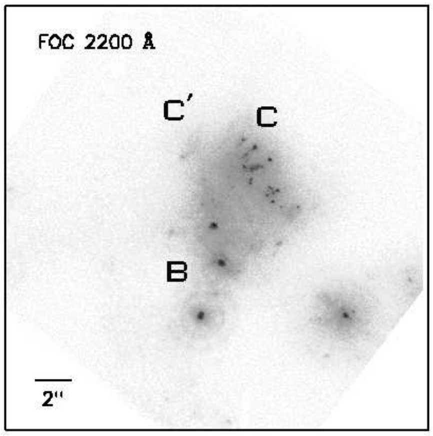

FIGURE 5. *HST FOC* 2200Å observation of the B-C-C′ complex in NGC 3690 (Arp 299 West) from Vacca 1995 [51]. These observations show that many of the massive stars in this system are confined to very bright, compact knots.

to compare the actual distributions and dynamics of the star forming regions and dense gas with the predictions of the simulations in order to discriminate between different numerical formalisms for star formation and gas dynamics. Only by doing this will we know how far to trust the models or how to better conduct our observations.

Other Aspects of Interaction Induced Starbursts

There are many other interesting aspects of interaction induced starbursts, and in the remaining space I simply mention a few.

Star Formation Knots: When viewed with sufficient resolution the star-forming regions in Arp 299 and NGC 4038/9 are found to break up into many distinct knots along with a diffuse component. Figure 5 shows an *HST FOC* image of NGC 3690 [50,51]. These knots have typical diameters of less than 10pc and may evolve into globular clusters [50,52]. However these knots are not unique to mergers [50,53–55], and it is not clear if this mode of star formation is increased in such interactions and if it is related to the enhanced SFE. It may just be an important mode of star formation in general. A detailed comparison of the luminosity functions of such knots from different types of environments would help resolve this question.

The Return of Tidal Debris: Due to the strong tides experienced during merging encounters, appreciable amounts of stars and gas are lifted high above the merging systems into tidal features. These features frequently exhibit significant substructure, the largest having observational properties typical of dwarf galaxies [56–59]. Much of this material remains bound to the remnant on long-period orbits, and will take several Gyr to fall-back [60,61]. Tidal clumps that are far out along the tails may be able to avoid tidal stripping when they fall back towards the remnant and should become long-lived dwarf companions [61], while the more tightly bound material will fall back into the remnant. The stellar component of these tails will wrap coherently in the central potential, giving rise to fine structure features [60] while the gas may feed a prolonged period of low-level star formation. The largest clumps have as much as a few $10^8 M_\odot$ of H I [58,59], and their return may give rise to smaller bursts. The overall star formation history in merger events should be similar to that illustrated by Worthy (this volume).

Because of the timescales and amounts of gas involved, we therefore do not expect two merging spirals to turn quickly into an elliptical, but rather for there to be a series of transitions, e.g. to an S0pec, to an S0, to a dust lane elliptical, etc. [59]. By the time the more obvious signs of its merger origin have faded and the remnant has evolved into a *bona fide* elliptical, the stars formed during the merger induced starburst will have aged 2-5 Gyr, leaving very little indication of a merger origin in the remnants broad band colors. This picture is quite similar to the one emerging from studies of cluster populations at high redshift (see Dressler, these proceedings).

Outstanding Questions

The main outstanding question for interaction induced star formation is the same as for any field of star formation: is the IMF universal, and if not how is it different in these violent environments? Are there upper and lower mass limits? Is the IMF top heavy? All of these effects have been claimed [30,62,63], but the observations allow for a wide range of parameters. A major problem with these determinations is that the observered bursts are both temporally and spatially variable, and as a result there will be a mix of burst populations of varying strength and ages spread throughout the merger. An IMF measured globally will reflect the luminosity averaged IMF over the region observed, which will be different in different wavebands. Careful UV and/or NIR spectroscopy of individual knots in conjunction with dynamical modeling should help separate these effects. Such observations should also help constrain the past star formation history in the systems, allowing one to map the age distribution of the star forming episodes.

Another major question is how does the energy injected back into the surrounding gas via the winds from massive stars and SNe change the gas dynamics and burst properties? This process, referred to as "feedback", is seen in its most extreme form in mergers, as evidenced by the galactic scale superwinds emerging from many ULIR systems (see Heckman, these proceedings). It may simply be an interesting side-effect of the circumnuclear star bursts, or it may dramatically affect the physics of star formation, for example by raising the lower-mass cutoff of the IMF or changing its high-end slope [64], or by regulating the star formation rate at some critical value [65].

There is much hope for further progress to be made in these areas in the future. It is becoming feasible to model a multi-phase ISM, which should help assess the importance of feedback. Further numerical trade studies should help decide how the different parameters interact and predict relationships between gaseous and star forming regions. Careful observations can test these predictions, and in this way we can discriminate between the different numerical formalisms. Not only will this provide a deeper understanding of interaction induced star formation, but ultimately it should be possible to decide which of the two histories depicted in Fig. 4 a merger follows, and which of these lead to an ULIR phase. Since the ULIR systems may be the closest analogs to the star forming galaxies seen at high redshift (see Madau, these proceedings), this understanding will provide valuable insight into the major processes at work during the epoch of galaxy formation.

I wish to thank J. van Gorkom and W. Vacca for comments on this manuscript; to M. Yun, C. Mihos, S. Aalto and W. Vacca for permission to reproduce their figures; and to the organizing comittee for setting up such an interesting meeting. This work is supported by Grant HF–1059.01–94A from STScI, which is operated by AURA, Inc., under NASA contract NAS5–26555.

REFERENCES

1. Zwicky, F. 1950, *Experientia*, 6, 441.
2. Burbidge, E.M., Burbidge, G.R., & Hoyle, F. 1963, ApJ, 138, 873.
3. Searle, L. Sargent, W.L.W., Bagnuolo, W.G. 1973, ApJ, 179, 427.
4. Larson, R.B., Tinsley, B.M. 1978 ApJ, 219, 46.
5. Arp, H.C. 1966, ApJ (Supp.), 14, 1.
6. Toomre, A., Toomre, J. 1972, ApJ, 178, 623.
7. Kennicutt, R.C.Jr. 1990, in "Paired and Interacting Galaxies", IAU Colloq. No. 124, Sulentic, Keel, & Telesco eds. (NASA, Washington), p. 269.
8. Bushouse, H.A., Lamb, S.A., & Werner, M.W. 1988, ApJ, 335, 74.
9. Sanders, D.B., *et al.* 1988, ApJ, 325, 74.
10. Keel, W.C., *et al.* 1985, AJ, 90, 708.
11. Bushouse, H.A. 1987, ApJ, 320, 49.
12. Kennicutt, R.C. Jr., *et al.* 1987, AJ, 93, 1011.
13. Condon, J.J., Huang, Z.-P, Yin, Q.F., Thuan, T.X. 1991, ApJ, 378, 65.
14. Lonsdale, C.J., Persson, S.E., Matthews, K. 1984, ApJ, 287, 95.
15. Joseph, R.D., Wright, G.S. 1985, MNRAS, 214, 87.
16. Arp, H., & Madore, B.F. 1975, Observatory, 95, 212.
17. Sanders, D.B., Mirabel, I.F. 1996, ARAA, 34, 749.
18. Condon, J.J. 1992, ARA&A, 30, 575.
19. Scoville, N.Z., *et al.* 1989, ApJ (Lett.), 345, L25.
20. Scoville, N.Z., Sargent, A.I., Sanders, D.B., Soifer, B.T. 1991, ApJ, 366, L5.
21. Lonsdale, C.J., Smith, H.E., & Lonsdale, C.J. 1995, ApJ, 438, 632.
22. Heckman, T.M. 1990, in "Paired and Interacting Galaxies", IAU Colloq. No. 124, Sulentic, Keel, & Telesco eds. (NASA, Washington), p. 357.
23. Young, J.S., Schloerb, F.P., Kenney, J.D., Lord, S.D. 1986, ApJ, 304, 443.
24. Solomon, P.M., Sage, L.J. 1988, ApJ, 334, 613.
25. Maloney, P. & Black, J.H. 1988, ApJ, 325, 389.

26. Downes, D., Solomon, P.M. & Radford, S.J.E. 1993, ApJ (Lett.), 414, L13.
27. Vigroux, L. *et al.* 1996, A&A, 314, L93.
28. Wynn-Williams, C.G., *et al.* 1991, ApJ, 377, 426.
29. Ridgeway, S.E., Wynn-Williams, C.G. & Becklin, E.E. 1994, ApJ, 428, 609.
30. Shier, L.M., Rieke, M.J. & Rieke, G.H. 1996, ApJ, 470, 222.
31. Hibbard, J.E., & Yun, M.S. 1996, in "Cold Gas at High Redshift", Bremer, Rottgering, van der Werf & Carilli eds. (Kluwer, Dordrecht), p. 47.
32. Aalto, S., Radford, S.J.E., Scoville, N.Z. & Sargent, A.I. 1997, ApJ, in press.
33. Stanford, S.A., Sargent, A.I., Sanders, D.B., Scoville, N.Z. 1990, ApJ, 349, 492.
34. Sargent, A.I., Scoville, N.Z. 1991, ApJ (Lett.), 366, L1.
35. Solomon, P.M., Downes, D., & Radford, S.J.E. 1992, ApJ (Lett.), 387, L55.
36. Kormendy, J. & Sanders, D.B. 1992, ApJ (Lett.), 390, L53.
37. Silk, J. 1996, ApJ, in press (astro-ph/9612117)
38. Elmegreen, B. 1994, in "Violent Star Formation from 30 Doradus to QSOs", ed. G. Tenorio-Tagel (Cambridge University Press, Cambridge).
39. Negroponte, J., White, S.D.M. 1983, MNRAS, 205, 1009.
40. Noguchi, M., Ishibashi, S. 1986, MNRAS, 219, 305.
41. Barnes, J.E., & Hernquist, L. 1991, ApJ (Lett.), 370, L65.
42. Barnes, J.E., & Hernquist, L. 1992, ARA&A, 30, 705.
43. Mihos, J.C., Hernquist, L. 1994, ApJ (Lett.), 431, L9.
44. Mihos, J.C., Hernquist, L. 1996, ApJ, 464, 641.
45. Hibbard, J.E., & Yun, M.S. in preparation.
46. van der Hulst, J.M. 1979, A&A, 155, 151.
47. Olson, K.M., Kwan, J. 1990, ApJ, 361, 426.
48. Augarde, R., and Lequeux, J. 1985, A&A, 147, 273.
49. Barnes, J.E., & Hernquist, L. 1996, ApJ, 471, 115.
50. Meurer *et al.* 1995, AJ, 110, 2665.
51. Vacca, W.D. 1995, "The Interplay between Massive Star Formation, the ISM, and Galaxy Evolution", Kunth *et al.* eds. (Ed. Frontieres) p. 321.
52. Whitmore, B.C. & Schweizer, F. 1995, AJ, 109, 960.
53. Conti, P.S. & Vacca, W.D. 1994, ApJ (Lett.), 423, L97.
54. Holtzman etal 1996, AJ, 112, 416.
55. Maoz, D., *et al.* 1996, AJ, 111, 2248.
56. Schweizer, F. 1978, "The Structure and Properties of Nearby Galaxies", IAU Symp. No. 77, Berkhuijsen and Wielebinski eds. (Reidel, Dordrecht), p. 279.
57. Mirabel, I.F., Duc, P.-A., & Dottori, H. 1994, in "Dwarf Galaxies", Meylan & Prugniel eds. (ESO) p. 371.
58. Hibbard, Guhathakurta, P., van Gorkom & Schweizer, F. 1994, AJ, 107, 67.
59. Hibbard, J.E., & van Gorkom, J.H. 1996, AJ, 111, 655.
60. Hernquist, L. & Spergel, D.N. 1992, ApJ (Lett.), 399, L117.
61. Hibbard, J.E., & Mihos, J.C. 1995, AJ, 110, 140.
62. Doyon, R., Puxley, P.J. & Joseph, R.D. 1992, ApJ, 397, 117.
63. Lançon, A. & Rocca-Volmerange, B. 1996, New Astronomy, 1, 215.
64. Zepf, S. & Silk, J. 1996, ApJ, 446, 114.
65. Lehnert, M.D. & Heckman, T.M. 1996b, ApJ, 472, 546.